Journal of Thermal Analysis and Calorimetry, Vol. 93 (2008) 2, 387–396

CHARACTERIZATION OF RICE HUSKS AND THE PRODUCTS OF ITS THERMAL DEGRADATION IN AIR OR NITROGEN ATMOSPHERE

S. D. Genieva[1], *S. Ch. Turmanova*[2], *A. S. Dimitrova*[2] *and L. T. Vlaev*[1*]

[1]Department of Physical Chemistry, Assen Zlatarov University, 8010 Bourgas, Bulgaria
[2]Department of Materials Science, Assen Zlatarov University, 8010 Bourgas, Bulgaria

Rice husk is a by-product of rice milling process and are a major waste product of the agricultural industry. They have now become a great source as a raw biomass material for manufacturing value-added silicon composite products, including silicon carbide, silicon nitride, silicon tetrachloride, pure silicon, zeolite, fillers of rubber and plastic composites, adsorbent and support of catalysts. The bulk and true densities of raw rice husk with different moisture and sizes were determined. The rice husk was subjected to pyrolysis in fluidized-bed reactor in air or nitrogen atmosphere.

The products obtained were characterized by thermogravimetric and X-ray powder analysis, IR-spectroscopy, scanning electron microscopy and nitrogen adsorption at 77 K. The specific surface area of the products is comparable with this of γ-Al_2O_3. The kinetics of H_2SeO_3 adsorption out of aqueous solutions at 298 K was studied. The adsorption capacity of white rice husks ash was found to be higher than that of black rice husk ash and the adsorption kinetics obeyed the second order kinetic equation.

Keywords: *black rice husks ash, DTA, IR analysis, pyrolysis, rice husks, thermal degradation, white rice husks ash, X-ray analysis*

Introduction

A number of reviews [1–6] have been dedicated to rice husks and the products obtained from its thermal degradation at different conditions. Large quantities of rice husks are available as waste from rice milling industry. According to the statistical data of Food and Agriculture Organization (FAO), the world annual paddy production is approximately 582 million tons. *Oryza sativa L*. husks (Rice husks) comprise 25 mass% of the rice grain and, therefore, 145 million tons of rice husks residue are produced [7]. These husks are not of commercial interest and cause serious pollution problems. It is necessary, then, to consider the use of this residue in polymer formulations with a clear positive effect to the environment. The chemical constituents are found to vary from sample to sample which may be due to the different geographical conditions, type of paddy, climatic variation, soil chemistry and fertilizers used in the paddy growth [4, 8–10]. The chemical analysis of these rice husks is found to be for instance 66.67% carbon, 22.3% SiO_2, 7.1% H_2O, 0.82% Al_2O_3, 0.78% Fe_2O_3, 1.10% K_2O, 0.78% Na_2O, 0.24% CaO and 0.21 mass% MgO [2, 4]. Because of its high silica and lignin content, rice husks are insoluble in water, tough, woody and abrasive in nature with low nutritive properties and resistance to weathering [11]. The silicon atoms are concentrated in the protuberances and hairs on the outer and inner epidermis of the husks in the predominant form of silica gel. The nature of silica is mainly amorphous and has been termed opaline silica [8]. The organic part is composed approximately of 42.8% cellulose, 22.5% lignin, 32.7% hemicellulose and other organic matter about 2%. Hemicellulose (xilan) is a mixture of *D*-xylose – 17.52%, *L*-arabinose – 6.53%, methylglucuronic acid – 6.53% and *D*-galactose – 2.37 mass% [2, 9]. These average values can change for different rice varieties.

It is well known that the rice husks have a low calorific value (3585 kcal kg^{-1}) and a high (20–22 mass%) ash content [5, 8, 9]. The ash contains nearly 95 mass% silica and is an important renewable source of silica. Burning is a cheap method of extracting the silica from rice husks for possible commercial use, but it brings up the associated problems of uncontrolled particle size and variable impurity levels, mainly in the form of intimately mixed carbon. Because of growing environmental concern and the need to conserve energy and resources, efforts have been made to burn the husks under controlled conditions and to utilize the residual ash in a variety of end products.

The controlled burning of the rice husks in air leads to production of white rice husk ash (WRHA) or so-called 'white ash' containing almost pure (≥95%) silica in a hydrated amorphous form, similar to silica gel, with high porosity and reactivity. This silica can be used as excellent starting materials for synthesis of

* Author for correspondence: vlaev@btu.bg

1388–6150/$20.00
© 2008 Akadémiai Kiadó, Budapest
Akadémiai Kiadó, Budapest, Hungary
Springer, Dordrecht, The Netherlands

advanced materials such as silicon tetrachloride [12], magnesium silicide [10], sodium silicate [13], zeolite [14, 15] etc. [16–18]. This silica is an excellent source of very high purity elemental silicon, useful for manufacturing solar cells for photovoltaic power generation and semiconductors [10, 19, 20]. White rice husk ash can be used also in the cement and fertilizer industries (as a pozzolone and as anti-caking component, respectively) [21–23].

The controlled pyrolysis of the raw rice husks (RRH) in nitrogen atmosphere leads to production of black rice husk ash (BRHA) or so-called 'black ash' which contains different amounts of carbon and silica. This material has very high porosity and may be used as a starting material for the synthesis of silicon carbide [24–26] and silicon nitride [10, 27]. Properties like high surface area and porosity give additional advantage to the WRHA and BRHA for their possible use adsorbents for adsorption of dyes, pigments [3, 6] and heavy metal ions [1, 5, 28] from aqueous solutions, catalytic support and catalyst [29–31]. In the recent years, the raw rice husk and rice husk ash are used as a fillers in rubber [32, 33] and plastic [34–36] composites, due to their low densities, very low cost, non-abrasiveness, high filling levels, recyclability, biodegradability and renewable nature.

The aim of the present paper is to characterize raw rice husks and black and white rice husk ash, the silica obtained from them and to study the possibilities to use the products for adsorption of ions from aqueous solutions.

Experimental

Rice husks were obtained from suburb areas of Thrace (Pazardjik, Bulgaria). Before use, the rice husks were thoroughly washed – three times with tap water followed by three times with deionised water to remove adhering soil, clay and dust, boiled for an hour to desorbs any impurities and finally, dried at 375±2 K overnight. The dried husks were ground in rotary cutting mill and sieved manually with 0.63–0.12 mm sieves. This starting material was used for all further studies. Bulk and true density of initial and grounded rice husks with different moisture were determined. Husk samples of different moisture contents were prepared in the following manner. The moisture content of husk was first increased from the initial value of 7.1 to 24.2 mass% by saturation with water vapour flow at 373 K for 4 h. The moisture content was determined by standard oven drying method (375 K for 24 h). Bulk densities of raw ungrounded and grounded rice husks were determined by loosely and uniformly filling 250 mL cylinder and weighing on analytical balance. The filling was performed by slowly pouring the material into the cylinder through a funnel without tapping. The true densities of raw and grounded rice husks were determined by the toluene displacement method, using pyknometer with volume of 50 mL.

The thermal treatment of the rice husk fraction with size 0.63–0.12 mm was carried out in quartz vertical tube equipped with perforated quartz diaphragm at its lower end. The electrical heater used was wound around the quartz tube and insulated by asbestos sleeve. During the thermal treatment, air or nitrogen was flown below the quartz diaphragm into the lower end of the tube (100 mL min^{-1}) through the treated material. The controlled increase of the temperature was performed using electronic thermal regulator Zeitplansolwertgeber, (Germany) at heating rate of 5 K min^{-1} up to 973 K, maintained for 2 h, after which the ash was quenched in air or nitrogen medium and used for further experiments.

Powder X-ray diffraction patterns of the samples were taken on a wide angle X-ray apparatus equipped with a goniometer URD-6 (Germany), using cells with a diameter of 12 mm, CuK_α radiation (λ=1.54 Å) and a nickel filter for β-emission. The scanning rate was 2° min^{-1}.

The IR absorption spectra were performed on a double beam spectrophotometer Specord-75 (Carl Zeiss-Jena, Germany) over the region from 400 to 4000 cm^{-1} (resolution 1 cm^{-1}), which was calibrated using a polystyrene film. The experiments were carried out at room temperature using the KBr disc technique. Approximately 1 mg of the sample were vigorously ground and mixed with 100–150 mg spectroscopically pure KBr powder by shaking for 15 s in a vibrator. The mixture was then compacted at about 15 MPa by means of a hydraulic press in a special die under vacuum.

The thermogravimetric analysis of the samples of 50 mg were performed on a Paulik–Paulik–Erdey-type Derivatograph thermobalance (MOM, Hungary) by heating to 1173 K at a heating rate of 10 K min^{-1} in a flow of air or nitrogen at a rate of 20 mL min^{-1}. The standard used was γ-Al_2O_3 heated to 1373 K. The TG, DTA and DTG curves were recorded simultaneously along with temperature rise. The curves were registered with resolutions 1/5 for DTA, 1/15 for DTG and 1 mg for TG.

The morphology of the samples was examined by a scanning electron microscope (SEM) Tesla BS 340 under regime of secondary electrons at acceleration of 20 kV. The samples were metallized with aluminum in Edwards 306 vacuum camera. The average thickness of the coating was measured to be 20 nm.

Surface properties of the samples were investigated by the adsorption of nitrogen at liquid nitrogen temperature (77 K), using a high vacuum

volumetric BET apparatus of the conventional type. Prior to experimental measurement, each sample was outgassed at 398±2 K for 4 h at a residual pressure about 10^{-6} Torr (1 Torr=133.32 Pa). For the characterization of the texture properties of the rice husk ash, the Brunauer–Emmett–Teller (BET) equation was derived [37]:

$$\frac{P_i/P_0}{\alpha_i(1-P_i/P_0)}=\left(\frac{c-1}{\alpha_m c}\right)\frac{P_i}{P_0}+\frac{1}{\alpha_m c} \quad (1)$$

where P_i/P_0 is the relative pressure, α_m is the capacity of monolayer and c is the BET constant, which is related to the molar energy of adsorption in the first monolayer. The specific surface area A_{BET} is a key parameter used to characterize the solids porous structure and its values were calculated by using the α_m value, which is easily determined from the linear equation above, according to the formula:

$$A_{BET}=\alpha_m N_A \omega \quad (2)$$

where N_A is the Avogadro's number and ω is the molecular cross-sectional area of adsorbate (0.1627 nm^2 for nitrogen). The single point total mesopore volumes $V_{0.95}$ obtained from the adsorption isotherms of nitrogen were calculated by the formula [37, 38]:

$$V_{0.95}=\alpha_{0.95}V_m \quad (3)$$

where $\alpha_{0.95}$ is the amount of adsorbate determined from the desorption branch of the isotherm at the relative pressure P_i/P_0=0.95 and V_m is the molar volume of liquid nitrogen which is known to be 34.68 mL mol^{-1}. The mean pore radius r_p was calculated using the follow ratio [37, 38]:

$$r_p=\frac{2V_{0.95}}{A_{BET}} \quad (4)$$

The kinetics of adsorption of H_2SeO_3 from aqueous solutions was studied using conductivity-meter InoLab WTW, (Germany) at temperature 298 K. The H_2SeO_3 concentration in the solution was measured by iodometric titration to be 0.0252 mol L^{-1}. The determination was carried out with 0.5000±0.0001 g of the samples and 50 mL H_2SeO_3 solution; the electric conductivity of the latter was measured at various time intervals. The measurements were based on the fact that, at T=const., the specific electrical conductivity of the solution (κ, S cm^{-1}) is a single-valued function of its concentration [39]. Then, in the definitive differential kinetic equation:

$$w=\pm\frac{dc}{dt}=kc^n \quad (5)$$

the solution concentration c may be replaced by the fraction adsorption α which is calculated according to the following relationship:

$$\alpha=\frac{\kappa_i-\kappa_\tau}{\kappa_i-\kappa_f} \quad (6)$$

where κ_i, κ_τ and κ_f are the initial, actual at the moment τ and final specific electric conductivities of the solution, respectively. Then, after proper integration, the following linear equation was obtained for first order reaction:

$$-\ln(1-\alpha)=k\tau \quad (7)$$

And for second order reaction (n=2) [40]:

$$(1-\alpha)^{-1}-1=k\tau \quad (8)$$

The value of the rate constant of adsorption k at certain temperature can be calculated from the slope of the straight line. The correlation coefficient of linear regression R^2 was used as criterion when estimating which one of the two equations describe better the kinetics of the process of adsorption.

Results and discussion

Since the pyrolysis of the rice husks is carried out most often in fluidized bed reactors, it is important to know the bulk and true densities of raw rice husks with different moisture and sizes for the assessment of the process hydrodynamics. Table 1 shows the data on the bulk and true densities of raw ungrounded and grounded rice husks with different moistures.

As can be seen from Table 1, the bulk density of ungrounded rice husks increased with the increase of moisture, whereas the bulk density of grounded density decreased. The bulk density of ground husk was found to be 2.38 to 2.84 times more than that of ungrounded rice husks. At the same time, the true density of ungrounded husks increased and that of grounded husks decreased. Thus, ground rice husks swell when moist. Density (bulk and true) of ungrounded

Table 1 Bulk and true density of ungrounded and grounded raw rice husks with different moisture

Moisture/ mass%	Bulk density/kg m^{-3}		True density/kg m^{-3}	
	ungrounded	grounded	ungrounded	grounded
7.1	101.2	287.8	1019	1502
24.2	105.5	251.6	1054	1456

husk increased with moisture content whereas the density of grounded husk decreased. The same tendency was observed by other authors [16], where it is pointed out that the relationship between the moisture content and true density is linear within the limits of the moisture content in both the ungrounded and grounded conditions of rice husks.

Figure 1 presents the photography of ungrounded raw rice husks and after its thermal treatment in nitrogen or in air atmosphere at 973 K.

It can be seen from Fig. 1 that the pyrolysis of rice husk RRH (Fig. 1a) in nitrogen medium gave BRHA (Fig. 1b), while the combustion in air gave – WRHA (Fig. 1c). These products are porous; they have high specific surface area and may be used as adsorbents for different compounds out of solutions.

The morphology of raw rice husk, black and white rice husk ash was examined by a scanning electron microscopy. SEM micrographs of raw rice husk, after combustion in air and after pyrolysis in nitrogen atmosphere at 973 K are presented in Fig. 2.

The main components of rice husk are in lemma and palea form, which tightly interlock with each other [41]. Figure 2 shows the outer epidermis of raw rice husk, which is well organized and has a corrugate structure. The outer surface of lemma is highly ridged, and the ridged structures have a linear profile. The epidermal cells of lemma are arranged in linear ridges and furrows, and the ridges are punctuated with prominent globular protrusions [2, 11, 17, 18, 41]. The outer surface of lemma also contains papillae and hairs of varying sizes, but they were often broken at their bases in the material examined, and therefore are not illustrated. As can be seen from Fig. 2a, the structure of raw rice husk was globular. The relatively stable Si–O carcass and biomass assembled around it formed the structure of rice hull. The silicon atoms are presented all over, but are concentrated in the protuberances and hairs (trichomes) on the outer and inner epidermis, adjacent to the rice kernel. After combustion of rice husk in air (Fig. 2b), the morphology tended to maintain its original shape although the product is brittle and loose when carefully pinched with the fingers. The only difference that can be observed was that the globules were shrinked and compacted due to the release of the volatile products. The hard residue was formed of almost pure SiO_2 (96.8 mass%). As it has been pointed out [17, 42], the rate of combustion process depends strongly on the vapor diffusion rate from the bulk of the spherical globules. The structure of the pyrolysis product obtained in nitrogen medium was also globular (Fig. 2c), but due to the lower percentage of volatile products released, the solid residue contained significantly more carbon (22.6 mass%). In this case, therefore, the initial globular structure of rice husk was also preserved due to the high thermal stability of SiO_2. The last two SEM micrographs showed that many residual pores are distributed within the ash samples, indicating that WRHA and BRHA is highly porous material with large internal specific surface area. The rice husk might have become broken up

Fig. 1 Appearance of ungrounded a – RRH, b – BRHA and c – WRHA

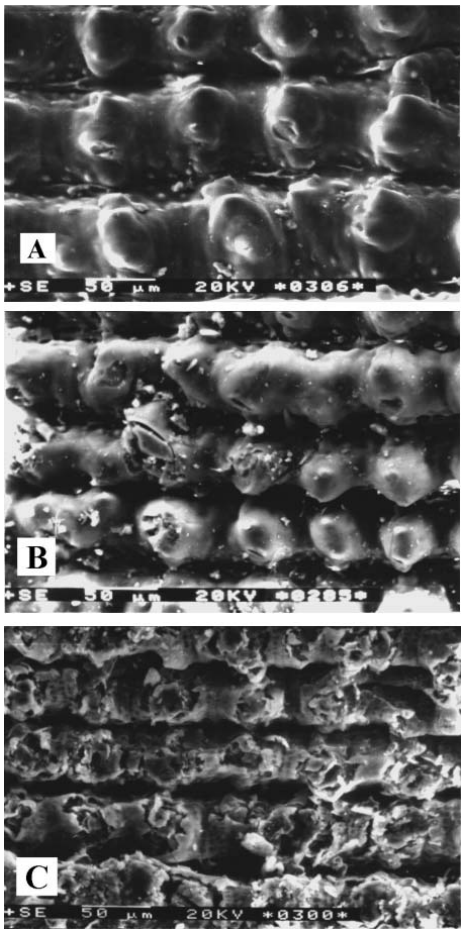

Fig 2 Scanning electron micrographs of ungrounded a – RRH, b – WRHA and c – BRHA at 973 K

during thermal decomposition of organic matter, thus obtaining highly porous structure. By comparison of these micrographs, it is observed that the surface of raw rice husk is relatively nonporous, whereas burned or pyrolyzed rice husk exhibit porous surface, as indicated by the pore structure analysis (nitrogen adsorption).

The pyrolysis of rice husk caused decomposition of organic part and breaking of the bonds with Si. The XRD patterns of the raw rice husks, pyrolyzed and combusted rice husks, as well as Aerosil A200 (Degussa AG, Germany), which is non-porous highly dispersed silica are shown on Fig. 3 for comparison.

Figure 3 shows X-ray diffraction analysis on rice husk before and after thermal degradation in nitrogen or air medium. All the three samples were amorphous, although a broad diffused peak centered at about $2\theta=22.5°$ was observed. No reflexes, characterizing cristobalite or tridymite phase were noticed in the samples studied, indicating the absence of any crystalline phases. Curve a from Fig. 3 represents the X-ray diffraction of the raw rice husk. A broad hump around $2\theta=23°$ was noticed, indicating the presence of amorphous silica (disordered cristobalite). The same results were obtained for the BRHA and WRHA, as well as for Aerosil (curve d) used for comparison. The maxima of the diffused peaks were found to vary from $2\theta=23°$ for raw rice husks to $2\theta=20.7°$ for white ash. This could be attributed to a gradual change in the bonding of silicon with organic material in raw rice husks to silica-silica bonding in white ash. According to [4, 18, 43, 44] the partially crystalline cellulose in naturally aged raw rice husks show an XRD peak at $2\theta=23.7°$. The XRD pattern for the raw rice husks, presented on Fig. 3 with its maximum at $2\theta=23°$ suggests that the silicon in raw rice husk is bonded with organic material. The pyrolyzed in nitrogen medium rice husks (curve b) showed an almost flat maximum spreading from $2\theta=21$ to 25.6°. Cristobalite was detected at temperature above 1000 K, while at 1423 K both cristobalite and tridymite were present. These results are in consistence with those obtained in other studies [9, 44, 45]. Aerosil Degussa used as reference has also amorphous structure similar to that of WRHA.

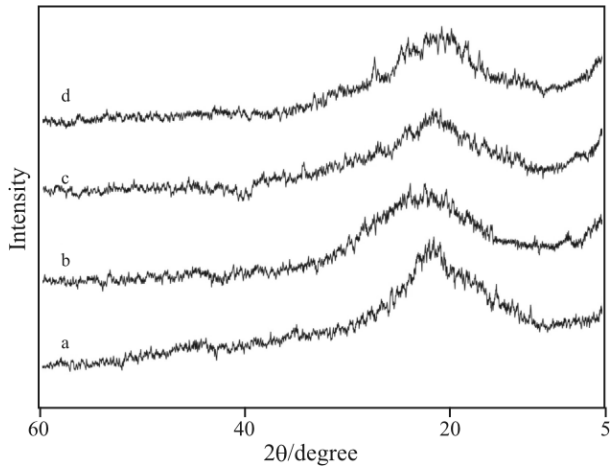

Fig. 3 X-ray diffraction patterns of: grounded a – RRH, b – BRHA, c – WRHA and d – Aerosil A200 Degussa

Going a little deeper into the structure of the organic compounds present in rice husks, the concept of the bonding of silicon with organic molecules can be confirmed. About the bonding of silicon with organic molecules, it may be said that cellulose $(C_6H_{10}O_5)_n$, being a polysaccharide and the main component of rice husk, does not seem to possess considerable bonding ability. Lignin, which coexists with cellulose, is mostly inert and therefore it is also not expected to be suitable for bonding. The remaining four organic components included in hemicellulose are aldehydes (monosaccharides), which become polar due to an electromeric effect. In the aldehyde group, the electromeric effect operates as shown below [17]:

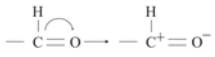

This type of electron transfer is brought into play only under the influence of an attacking reagent. The nature of silicon bonding in rice husk is complex and it appears to be bonded with the carbohydrates only. The possible bonding of silicon with four aldehyde residues in the raw rice husk, as indicated above, may be illustrated with the following scheme [17, 44]:

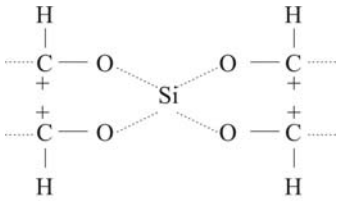

The different groups in which silicon exists, e.g. siloxane Si–O and silanol Si–OH, are best observed in IR spectra. Figure 4 presents IR absorption spectra of raw rice husks after pyrolysis in nitrogen or combustion in air at 973 K and for comparison – Aerosil A200 (Degussa AG, Germany).

Infrared spectroscopy provides information on the chemical structure and surface functional groups of the samples. It can be seen from Fig. 4 (spectrum a) that raw rice husks are characterized by broadband between 3700 and 3000 cm^{-1}. The intense absorption band with maximum about 3438 cm^{-1} can be attributed either to the stretching vibrations of O–H bonds in water molecules, bonded by hydrogen bonds, or to OH groups presented in cellulose, hemicellulose and lignine [9–11, 25, 46–48]. The band at 1620 cm^{-1} correspond to the deformation vibrations of water molecules (δ-H_2O). The position and asymmetry of

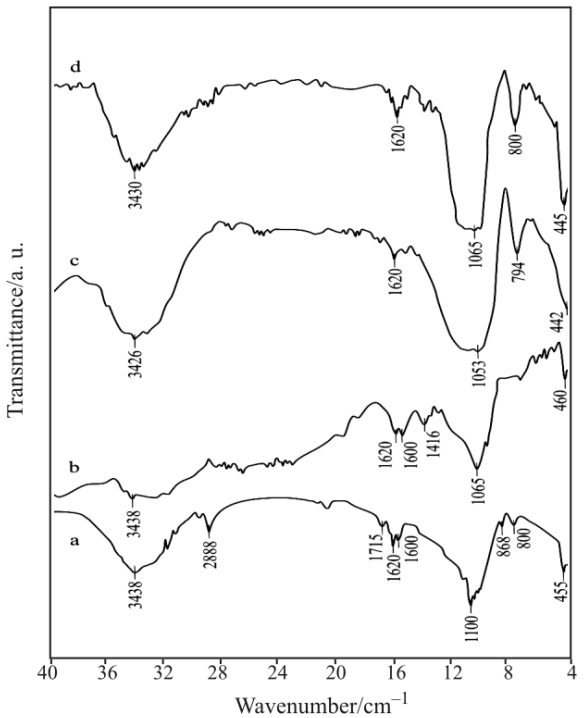

Fig. 4 IR absorption spectra of a – RRH, b – BRHA, c – WRHA and d – Aerosil A200 Degussa

these bands at lower wave numbers indicate the presence of strong hydrogen bonds. The intense adsorption band observed at 2888 cm^{-1} and the less intense band at 2900 cm^{-1} can be attributed to the symmetric (ν_s) and asymmetric (ν_{as}) stretching vibrations of the aliphatic C–H bonds in –CH_3 and CH_2 groups in the structures cellulose, hemicellulose and lignine, respectively. The very small peak at 1715 cm^{-1} was related to the C=O stretching vibrations of the bonds in the aldehyde groups of hemicellulose. The triplet in the IR spectra of raw rice husk in the region 1200–1000 cm^{-1} was considered to result from superposition of vibrations of the C–OH bond and Si–O bond in the siloxane (Si–O–Si) groups. The intense band at 1100 cm^{-1} corresponds to the stretching vibrations of silicon–oxygen tetrahedrons – $\nu_{as(SiO_4)}$. The high intensity of this peak was probably due to superposition of the stretching vibrations of the C–OH bond in the interval 1200–1000 cm^{-1} and the stretching vibrations of the Si–O bond. The weak absorption bands at 868 and 800 cm^{-1} can be explained with the symmetric and asymmetric vibrations of the Si–O bonds in the silicon–oxygen network. The absorbance peak at 455 cm^{-1} was due to the bending vibration (δ_{as}) of siloxane bonds.

After the pyrolysis of rice husk in nitrogen medium, the IR spectrum (spectrum b) of the black ash obtained did not differ significantly from that of raw rice husks, except for the quite higher intensities of the bands at 1065 and 460 cm^{-1}. This can be explained with the decrease of organic matter content and its transformation into active carbon. The thermal treatment of rice husk in air, however, resulted in very different IR spectrum (Fig. 4, spectrum c). Wide, highly intense peak was observed with maximum at 3426 cm^{-1}, attributed to the stretching vibrations of silanol groups. The bands at 1053 and 794 cm^{-1} correspond to the Si–O stretching vibration and the bending vibration at 442 cm^{-1} appeared sharper as the organic matter was no longer present. The positions of this feature are the same as those observed for commercial grade silica. Probably, the silicon atom was initially attached to the oxygen atom in raw rice husk and, after the thermal decomposition, the combination of silicon and oxygen atoms lead to the formation of amorphous silica. In addition, it can be also observed that the peak for the white ash sample was sharper peak than that of the black ash sample, indicating that the percentage of silica contents increased when the rice husk is burnt in air. The IR spectrum of white rice husk ash silica is the same as those of Aerosil A200 Degussa.

According to the data obtained from thermogravimetric analysis, the thermal decomposition of rice husks in air medium occurred in three main stages of mass loss, namely, removal of moisture (drying); release of organic volatile matters (devolatilization) and oxidation of fixed carbon (slow combustion) [4, 42, 49, 50]. TG and DTG curves of studied samples are presented in Fig. 5.

As can be seen from Fig. 5, curve a, the mass loss in the first stage took place in the range 350–423 K and is accompanied with small endothermic effect. The mass loss is about 7% and it is associated with the evolution of adsorbed water in the sample and external water bonded by surface tension. The observed features of the thermal decomposition of rice husks can be explained on the basis of the decomposition behaviors of its major constituents: cellulose, hemicellulose, lignin and ash. Mansaray and Ghaly [42] reported that the hemicellulose and cellulose components of the rice husk were the main contributors to the evolution of the volatile compounds, while lignin is mainly responsible for the char portion of the product. According to Stefany *et al.* [7] hemicellulose is degraded first at temperatures between 423 and 623 K, cellulose from 548 to 653 K and finally lignin from 523 to 823 K. The second and major mass loss of nearly 50% is attributed to the breakdown of the cellulose constituent to combustible volatiles, water, carbon dioxide and char. Using a pyknometer as described previously, the true densities of the white and black rice husk ash were measured to be 2200 and 1800 kg m^{-3}, respectively. It is considerably more than the true density of grounded

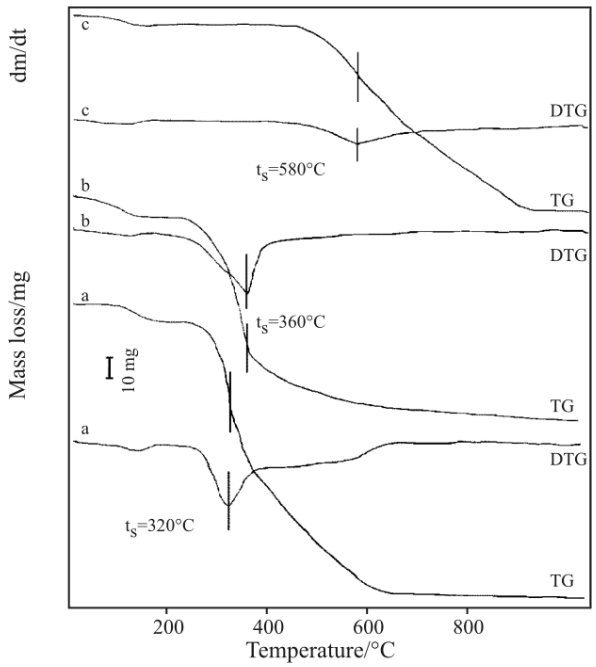

Fig. 5 TG and DTG curves of the samples: a – combustion in air of grounded rice husks, b – pyrolysis in nitrogen flow and c – burning in airflow of carbonized rice husks

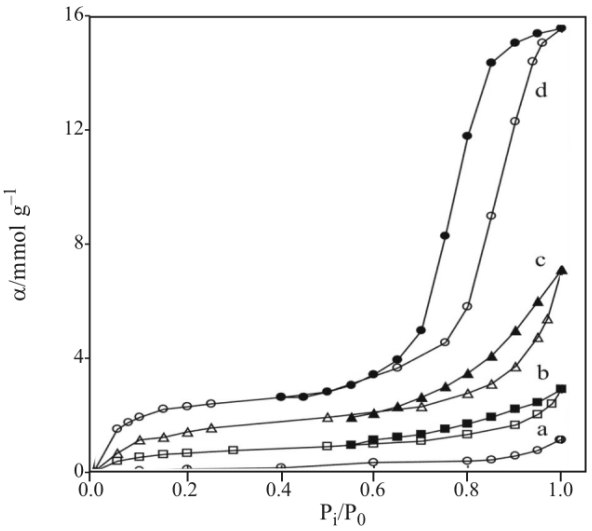

Fig. 6 Nitrogen adsorption-desorption isotherms at 77 K of grounded a – RRH, b – BRHA, c – WRHA and d – γ-Al_2O_3; ○, △, □ – adsorption, ●, ▲, ■ – desorption branch

raw rice husk. The lower density of the latter was due to the high content of active carbon in it (≥20%).

The kinetic mechanism and kinetic parameters of non-isothermal degradation of rice husks in nitrogen or air medium have been described in detail in [51, 52]. The smaller kinetic parameters obtained in the third stage, compared to these obtained in second stage, may be due to the fact that lignin, which has lower decomposition rates than cellulose and hemicellulose components in rice husk, was condensed to char.

Figure 6 shows the adsorption-desorption isotherms of nitrogen obtained with raw rice husk, BRHA, WRHA and for comparison – γ-Al_2O_3 from Leuna (Germany).

Figure 6 (curve a) shows no obvious hysteresis loop for the raw rice husk. Besides, the adsorption isotherm is convex over the entire range, indicating that the forces of adsorption between adsorbate and adsorbent are relatively weak. This adsorption isotherm is type III according to Brunauer–Deming–Deming–Teller classification [37, 38]. The quite low adsorption capacity within the whole range of relative pressures studied suggests very low values of the specific area and volume of the pores. The thermal treatment of rice husk in nitrogen and especially in air gave increased adsorption capacity of the samples and formation of high porosity (curves b and c). The adsorption isotherms are type IV according to the same classification. At low values of P_i/P_0, the isotherms are similar to type II but adsorption increases markedly at P_i/P_0 above 0.4 where pore condensation takes place. These results indicate that the rice husk ash is porous material [4, 48, 53, 54]. The characteristic shape of a type IV isotherm is the result of surface coverage of the mesopore walls followed by pore filling and it is associated with various hysteresis loops. The hysteresis loops (associated with capillary condensation) found in both samples are of H1 type of IUPAC classification [37]. A narrow type H1 hysteresis loop, with almost vertical and parallel branches, is generally associated with delayed condensation and very little percolation hold-up. The difference between isotherm b, c and a indicates that pore opening takes place when the rice husk is burned in air or carbonized in nitrogen atmosphere, which is probably related to the conversion of silanol groups into siloxane bridges. The γ-Al_2O_3 used for comparison is characterized by typical isotherm type IV, hysteresis loop type H1 and adsorption capacity quite higher than that of thermally treated rice husk. The results obtained for nitrogen adsorption, BET surface area, total pore volume and average pore radii are presented in Table 2.

As can be seen from Table 2, raw rice husk is characterized by very low specific area and pore volume, i.e. they practically do not have micro- and mesoporous structure. Comparing the porous structure of BRHA and WRHA, the latter was found to have higher specific area, volume and average radius of pores. The reason for this is that the whole quantity of carbon in rice husk has been burnt and the residue is practically pure SiO_2 with porous structure similar to that of silica gel. The reference γ-Al_2O_3, however, has much larger specific surface area and pore volume. This was considered enough to suggest that the thermal

Table 2 Characteristics of the porous structure of the samples studied

Sample	A_{BET}/m^2 g^{-1}	$V_{0.95}$/mL g^{-1}	r_p/nm
Raw rice husks	<1	<0.01	–
BRHA	96	0.185	3.6
WRHA	126	0.208	8.9
γ-Al_2O_3	162	0.534	6.5

treated rice husks would have lower adsorption ability. Taking into account the fact that the SiO_2 surface is polar due to the presence of surface OH groups while that of SiO_2/C is much less polar, different ion-exchange abilities of these two products should be expected. In this respect, certain information can be obtained from studies on adsorption of H_2SeO_3 from aqueous solutions. Since H_2SeO_3 behaves like weak electrolyte (K_1=2.4·10^{-3} and K_2=4.8·10^{-9} at 298 K), the solution contains both molecules and ions of selenous acid produced by its dissociation (Scheme I) [39]:

$$H_2SeO_3 \rightarrow H^+ + HSeO_3^- \qquad \text{(Scheme I)}$$

The ion-exchange reaction on the silica surface is accomplished through the substitution of OH groups of the surface silanol groups by the hydrogen-selenite anions from solution, as follows:

$$\equiv Si{-}OH + HSeO_3^- \rightarrow \equiv Si{-}O{-}Se(=O)(OH) + OH^-$$

Scheme II

OH^- ions obtained bond with H^+ ions to produce H_2O so the specific electric conductivity of the solution at certain moment is determined only by the ions resulting from Sceme I. Since adsorption equilibrium is reached after certain period according to Scheme II, then the electric conductivity of the solution should remain constant when equilibrium is reached. Therefore, the change of the solution specific electric conductivity with time at given temperature can be used to study the kinetics of H_2SeO_3 adsorption from aqueous solutions on various adsorbents [55]. In this respect, the curves describing the change of the specific electric conductivity of H_2SeO_3 solutions with time at 298 K in presence of various adsorbents (γ-Al_2O_3, BRHA and WRHA) are presented on Fig. 7.

At constant temperature (298 K), initial H_2SeO_3 concentration (0.0252 mol L^{-1}), solution volume (50 mL) and adsorbent mass (0.5000±0.0001 g), the change of the specific electric conductivity of the solution κ with time depends only on the adsorption ability of the samples studied. Therefore, the shape of the kinetic curves would reflect the porous structure of the adsorbent and polar nature of its surface.

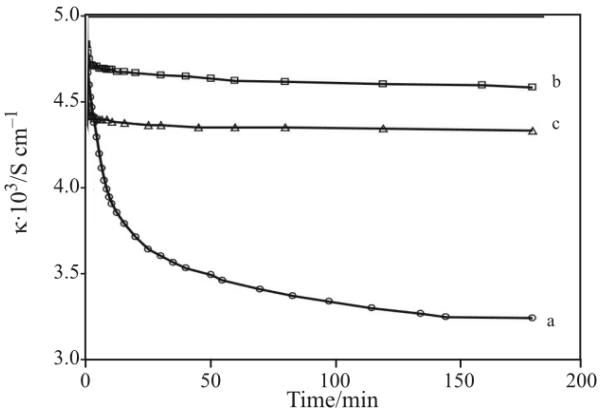

Fig. 7 Kinetic curves of sorption of H_2SeO_3 out of aqueous solution at 298 K on: a – γ-Al_2O_3, b – BRHA and c – WRHA

Comparing curves a and b from Fig. 7, it may be concluded that the sample obtained after combustion in air (WRHA) showed bigger decrease of solution electric conductivity and, therefore, its adsorption ability towards H_2SeO_3 was higher than that of the sample obtained after pyrolysis of rice husks in nitrogen atmosphere (BRHA). This difference may be attributed to the polar nature of SiO_2 surface in WRHA and the reaction (II) occurring on it. This was confirmed by the thrice-higher adsorption ability of γ-Al_2O_3, which also has highly polar surface due to the surface hydroxyl groups. The second reason for this observation is the significantly larger specific surface area of γ-Al_2O_3 and its accessibility for adsorbate molecules. The kinetic lines calculated according to the kinetic equation assumed to describe better the experimental data are presented in Fig. 8.

The experimental data were best described by a kinetic equation for second order reaction (Eq. (8)). The values of the correlation coefficient of linear regression R^2, rate constant k, maximal adsorption capacity α_{max} and equilibrium percentage of adsorption A are presented in Table 3.

The low values of the rate constant and adsorption capacity observed by the adsorption of H_2SeO_3 on BRHA were due to the lower specific area and comparatively small pore radius, as well as the non-polar character of the adsorbent surface. The quite higher value of the rate constant of the adsorption on WRHA can be attributed to the higher pore radius and specific area, as well as the strong polarity of the adsorbent surface generated by the OH groups. γ-Al_2O_3 had the highest adsorption capacity towards H_2SeO_3 molecules since it has the largest specific area with the highest polarity. As can be seen from Table 3, the value of the rate constant of the adsorption of H_2SeO_3 on γ-Al_2O_3 was higher than that for BRHA and lower than that for WRHA. It can be explained with pore radius, which turned out to be between these of BRHA and WRHA.

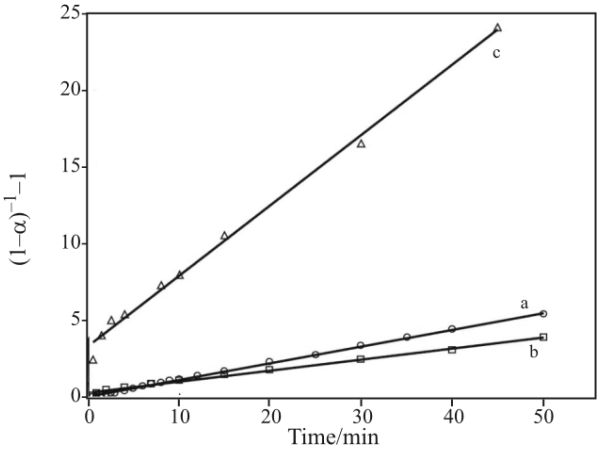

Fig. 8 Plot of $(1–\alpha)^{-1}–1$ *vs*. time for adsorption of H_2SeO_3 out of aqueous solution on: a – γ-Al_2O_3, b – BRHA and c – WRHA

Table 3 Adsorption of H_2SeO_3 out of aqueous solutions at 298 K

Parameter	BRHA	WRHA	γ-Al_2O_3
R^2	0.9938	0.9946	0.9987
k/min^{-1}	0.0715	0.4541	0.1091
α_{max}/mmol g^{-1}	0.1080	0.2081	0.6968
A/%	1.39	2.68	8.98

Therefore, it can be concluded that the pore radius, while the adsorption capacity – determines the adsorption kinetics by the size and polar nature of adsorbent's specific surface. γ-Al_2O_3 has the highest adsorption capacity because of the polar nature and large size of its specific area but the adsorption was lower because of the smaller pore size. Taking into account the much lower price of WRHA compared to γ-Al_2O_3, it can be concluded that WRHA can successfully be used for adsorption of H_2SeO_3 from various wastewaters. The advantage in the application of rice husk ash as an adsorbent is that there is no need to regenerate them because of their low production cost.

Conclusions

The method of thermal treatment of raw rice husks helps to solve the disposal and pollution problems of the rice milling industry and give an excellent starting materials for preparation of advanced high-quality ceramic powders, such as silicon carbide, silicon nitride and magnesium silicide, which are good for application in high temperature material engineering, especially for turbine engines. In addition, small scale of pure silica powder can be widely used for production of high purity elemental silicon for electronic, adsorbents, catalyst support, as tixotropic agents, thermal insulator and filler of rubbers and plastics, etc. [56].

References

1 S. E. Bailey, T. J. Olin, R. M. Bricka and D. D. Adrian, Water Res., 33 (1999) 2469.
2 S. Chandrasekhar, K. G. Satyanarayana, P. N. Pramada, P. Raghavan and T. N. Gupta, J. Mater. Sci., 38 (2003) 3159.
3 S. Babel and T. A. Kurniawan, J. Hazard. Mater., B97 (2003) 219.
4 T. H. Liou, Carbon, 42 (2004) 785.
5 T. G. Chuah, A. Jumasiah, I. Aznu, S. Katayon and S. Y. Thomas Choong, Desalination, 175 (2005) 305.
6 G. Crini, Bioresource Technol., 97 (2006) 1061.
7 P. M. Stefany, D. Garcia, J. Lopez and A. Jimenez, J. Therm. Anal. Cal., 81 (2005) 315.
8 D. S. Chaudhary and M. S. Jollands, J. Appl. Polym. Sci., 93 (2004) 1.
9 I. G. Markovska and L. A. Lyubchev, J. Therm. Anal. Cal., 89 (2007) 809.
10 S. Chandrasekhar, P. N. Pramada L. Praveen, J. Mater. Sci., 40 (2005) 6535.
11 A. A. M. Daifullah, B. S. Girgis and H. M. H. Gad, Mater. Lett., 57 (2003) 1723.
12 E. S. M. Seo, M. Andreoli and R. Chiba, J. Mater. Proc. Technol., 141 (2003) 351.
13 N. Sekar and T. Virutha Giri, Chem., Eng. World, 40 (2005) 81.
14 A. K. Dalal, M. S. Rao and K. V. G. K. Gokhale, Ind. Eng. Chem. Prod. Res. Dev., 24 (1985) 465.
15 M. Chareonpanich, T. Namto, P. Kongkachuichay and J. Limtrakul, Fuel Proc. Technol., 85 (2004) 1623.
16 P. Misra, A. Chakraverty and H. D. Banerjee, J. Mater. Sci., 21 (1986) 2129.
17 M. Patel, A. Karera and P. Prasanna, J. Mater. Sci., 22 (1987) 2457.
18 C. Real, M. D. Alcala and J. M. Criado, J. Am. Ceram. Soc., 79 (1996) 2012.
19 L. P. Hunt, J. P. Dismukes, J. A. Amick, A. Schei and K. Larsen, J. Electrochem. Soc., 131 (1984) 1683.
20 L. Sun and K. Gong, Ind. Eng. Chem. Res., 40 (2001) 5861.
21 V. I. E. Ajiwe, C. A. Okeke and F. C. Akigew, Bioresour. Technol., 73 (2000) 37.
22 R. Jauberthie, F. Rendell, S. E. Tamba and I. K. Cisse, Constr. Build. Mater., 17 (2003) 239.
23 E. A. Basha, R. Hashim and A. S. Muntohar, Electronic J. Geotech. Eng., 8A (2003) 827.
24 R. V. Krishnarao, Y. R. Mahajan and T. J. Kumar, J. Eur. Ceram. Soc., 18 (1998) 147.
25 K. Sujirote and P. Leangsuwan, J. Mater. Sci., 38 (2003) 4739.
26 V. Rodriguez-Lugo, E. Ribio, I. Gomez, L. Torres-Martinez and V. M. Castano, Int. J. Environ. Pollution, 18 (2002) 378.
27 C. Real, M. D. Alcala and J. M. Criado, J. Am. Ceram. Soc., 87 (2004) 75.
28 M. M. D. Zulkali, A. L. Ahmad and N. H. Norulalmal, Biores. Technol., 97 (2006) 21.
29 M. T. Tsai and F. W. Chang, Appl. Catal., A: General, 203 (2000) 15.
30 F. W. Chang, W. Y. Kuo and H. C. Yang, Appl. Catal. A: General, 288 (2005) 53.
31 F. W. Chang, H. C. Yang, L. S. Roselin and W. Y. Kuo, Appl. Catal. A: General, 304 (2006) 30.

32 H. Ismail, J. M. Nizam and H. P. S. Khalil, Polym. Test., 20 (2001) 125.
33 W. Arayapranee, N. Naranong and G. L. Rempel, J. Appl. Polym. Sci., 98 (2005) 34
34 D. S. Chaudhary, M. C. Jollands and F. Cser, Silicon Chem., 1 (2002) 281.
35 H. G. B. Premalal, H. Ismail and A. Baharin, Polym. Test., 21 (2002) 833.
36 S. Siriwardena, H. Ismail, U. S. Ishiaku and M. C. S. Perera, J. Appl. Polym. Sci., 85 (2002) 438.
37 S. J. Gregg and K. S. W. Sing, Adsorption, Surface Area and Porosity, 2nd Ed., Academic Press, New York 1982.
38 P. Tanev and L. Vlaev, J. Col. Int. Sci., 160 (1993) 110.
39 L. Vlaev, M. Tavlieva and M. Bester-Rogac, J. Sol. Chem., 36 (2007) 171.
40 L. Vlaev and M. Tavlieva, J. Therm. Anal. Cal., 90 (2007) 385.
41 B. D. Park, S. G. Wi, K. H. Lee, A. P. Singh, T. H. Yoon and Y. S. Kim, Biomass Bioenergy, 25 (2003) 319.
42 K. G. Mansaray and A. E. Ghaly, Biomass Bioenergy, 17 (1999) 19.
43 T. H. Liou, Mater. Sci. Eng., A346 (2004) 313.
44 R. V. Krishnarao and M. M. Gotkhindi, Ceram. Int., 18 (1992) 243.
45 M. A. Hamad and I. A. Khattab, Thermochim. Acta, 48 (1981) 343.
46 D. M. Ibrahim, S. A. El-Hemaly and F. M. Abdel-Kerim, Thermochim. Acta, 37 (1980) 307.
47 J. J. M. S. Rao, Thermochim. Acta, 97 (1986) 329.
48 T. H. Liou, Mater. Sci. Eng., A346 (2004) 313.
49 A. Chakraverty, P. Mishra and H. D. Banerjee, Thermochim. Acta, 94 (1985) 267.
50 H. R. Yuan and R. H. Liu, J. Therm. Anal. Cal., 89 (2007) 983.
51 A. Sharma and T. R. Rao, Biores. Technol., 67 (1999) 53.
52 L. T. Vlaev, I. G. Markovska and L. A. Lyubchev, Thermochim. Acta, 406 (2003) 1.
53 S. Hanafi, S. A. Abo-El-Enein, D. M. Ibrahim and S. A. El-Hemaly, Thermochim. Acta, 37 (1980) 137.
54 C. H. Yun, Y. H. Park and C. R. Park, Carbon, 39 (2001) 559.
55 L. Vlaev and S. Genieva, Russ. J. Phys. Chem., 78 (2004) 23.
56 S. Ch. Turmanova, S. D. Genieva, A. S. Dimitrova and L. T. Vlaev, Express Polym. Lett., 2 (2008) 133.

Received: August 9, 2007
Accepted: February 19, 2008

DOI: 10.1007/s10973-007-8429-5